Fighting against Drug-Resistant Tumors using a Dual-Responsive Pt(IV)/Ru(II) Bimetallic Polymer

Xiaolong Zeng, Yufei Wang, Jianxiong Han, Wen Sun, Hans-Jürgen Butt, Xing-Jie Liang,* and Si Wu*

Drug resistance is a major problem in cancer treatment. Herein, the design of a dual-responsive Pt(IV)/Ru(II) bimetallic polymer (PolyPt/Ru) to treat cisplatin-resistant tumors in a patient-derived xenograft (PDX) model is reported. PolyPt/Ru is an amphiphilic ABA-type triblock copolymer. The hydrophilic A blocks consist of biocompatible poly(ethylene glycol) (PEG). The hydrophobic B block contains reduction-responsive Pt(IV) and red-light-responsive Ru(II) moieties. PolyPt/Ru self-assembles into nanoparticles that are efficiently taken up by cisplatin-resistant cancer cells. Irradiation of cancer cells containing PolyPt/Ru nanoparticles with red light generates $^1O_2$, induces polymer degradation, and triggers the release of the Ru(II) anticancer agent. Meanwhile, the anticancer drug, cisplatin, is released in the intracellular environment via reduction of the Pt(IV) moieties. The released Ru(II) anticancer agent, cisplatin, and the generated $^1O_2$ have different anticancer mechanisms; their synergistic effects inhibit the growth of drug-resistant cancer cells. Furthermore, PolyPt/Ru nanoparticles inhibit tumor growth in a PDX mouse model because they circulate in the bloodstream, accumulate at tumor sites, exhibit good biocompatibility, and do not cause side effects. The results demonstrate that the development of stimuli-responsive multi-metallic polymers provides a new strategy to overcome drug resistance.

Cisplatin and various other Pt(II) anticancer drugs are administered to the majority of patients undergoing chemotherapy.[1,2] The development of drug resistance during chemotherapy treatment is a major problem; cisplatin becomes inefficient in patients after extended use.[3,4] Cisplatin resistance is due to multiple deactivation pathways that render the treatment

inefficient.[1] First, proteins such as serum albumin in blood deactivate cisplatin.[5] Second, cisplatin cannot be efficiently taken up by cisplatin-resistant cancer cells.[6] Third, intracellular biomolecules such as metallothionein (MT) and glutathione (GSH) may strongly bind and sequester cisplatin.[7] Fourth, the DNA of cancer cells that are damaged by cisplatin, can be repaired by proteins.[8] All these deactivation pathways hinder the curative effects of cisplatin.

Some strategies have been developed to overcome the abovementioned deactivation pathways. For example, Pt(IV) prodrugs, which release cisplatin in cancer cells, have been developed.[9–12] Pt(IV) prodrugs are more resistant to ligand substitution reactions than cisplatin because Pt(IV) centers are saturated and kinetically more inert.[1] Thus, Pt(IV) can minimize unwanted side reactions with biomolecules prior to DNA binding. Another strategy to overcome deactivation is to combine cisplatin with other anticancer agents such as paclitaxel, 5-fluorouracil, gemcitabine or ruthenium complexes.[13–16] Mixtures of anticancer agents possess multiple targets and actions; this strategy strengthens the therapeutic effects via the different anticancer mechanisms of the different agents.[14] A third strategy to overcome deactivation is to use nanocarriers for the delivery of cisplatin.[17,18] Some

X. Zeng, J. Han, Prof. S. Wu
CAS Key Laboratory of Soft Matter Chemistry
Hefei National Laboratory for Physical Sciences at the Microscale
Department of Polymer Science and Engineering
University of Science and Technology of China
Hefei 230026, China
E-mail: siwu@ustc.edu.cn
X. Zeng, J. Han, Prof. H.-J. Butt, Prof. S. Wu
Max Planck Institute for Polymer Research
Ackermannweg 10, Mainz 55128, Germany

iD The ORCID identification number(s) for the author(s) of this article can be found under https://doi.org/10.1002/adma.202004766.

Y. Wang, Prof. X.-J. Liang
Chinese Academy of Sciences (CAS) Key Laboratory for Biomedical
Effects of Nanomaterials and Nanosafety
CAS Center for Excellence in Nanoscience
National Center for Nanoscience and Technology
Beijing 100190, China
E-mail: liangxj@nanoctr.cn
Y. Wang, Prof. X.-J. Liang
University of Chinese Academy of Sciences
Beijing 100049, China
Dr. W. Sun
State Key Laboratory of Fine Chemicals
Dalian University of Technology
2 Linggong Road, Hi-Tech Zone, Dalian 116024, China

**ADVANCED
SCIENCE NEWS**
www.advancedsciencenews.com
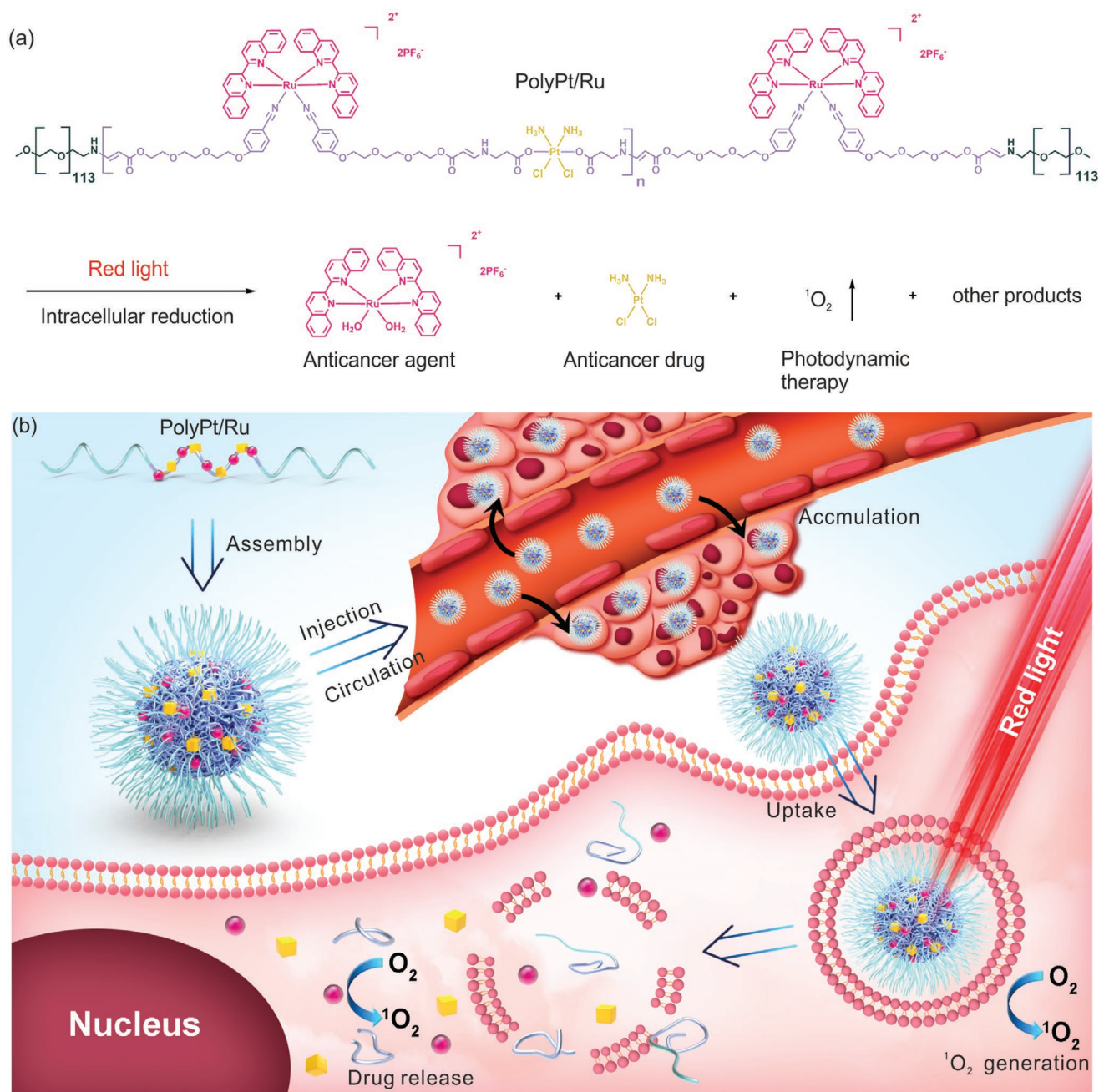
**ADVANCED
MATERIALS**
www.advmat.de

Figure 1. a) Structure of the amphiphilic triblock copolymer PolyPt/Ru. Red light irradiation and intracellular reduction induced degradation of the polymer, generation of $^1O_2$, and release of the anticancer drug cisplatin and the anticancer agent $[Ru(biq)_2(H_2O)_2](PF_6)_2$ (biq = 2,2'-biquinoline). b) Schematic illustration of self-assembly, extracellular and intracellular processes for anticancer therapy using PolyPt/Ru.

nanocarriers can circulate longer in the bloodstream, accumulate at tumor tissue via the enhanced permeation and retention (EPR) effect, be taken up by tumor cells efficiently, and release Pt drugs on demand.[19–22] These properties of nanocarriers can prevent deactivation pathways. Although the abovementioned strategies prevented certain deactivation pathways for cisplatin, it is difficult to overcome multiple deactivation pathways. Thus, reversing cisplatin resistance poses a challenge.

Herein, the design of a dual-responsive Pt(IV)/Ru(II) bimetallic polymer PolyPt/Ru to overcome multiple deactivation

pathways for cisplatin is reported. We demonstrated the use of PolyPt/Ru for the treatment of cisplatin-resistant tumors in a patient-derived xenograft (PDX) mouse model (**Figure 1**). PolyPt/Ru is an ABA-type triblock polymer with a hydrophobic Pt(IV)/Ru(II) bimetallic block and two hydrophilic poly(ethylene glycol) (PEG) blocks. The Pt(IV) moieties in the hydrophobic block are prodrugs that produce cisplatin in intracellular reduction environments. The Ru(II) moieties were incorporated in the hydrophobic block because some Ru(II) complexes show anticancer activity and have entered clinical trials.[23,24]

ADVANCED
SCIENCE NEWS

www.advancedsciencenews.com

ADVANCED
MATERIALS

www.advmat.de

In particular, some Ru(II) complexes can generate $^1O_2$ and undergo ligand substitution under light irradiation.[25–30] Photocaged Ru(II) complexes are usually nontoxic to nonirradiated tissues and can become toxic in cancer cells through photoactivation.[24,29] This photoactivation strategy can improve selectivity in cancer treatment. The Ru(II) moieties in PolyPt/Ru can generate $^1O_2$ for photodynamic therapy (PDT) and release anticancer Ru(II) complexes for photoactivated chemotherapy (PACT). Additionally, we used the hydrophilic and biocompatible PEG block because it can prolong blood circulation and suppress nonspecific adsorption of proteins that deactivate metallodrugs.[31–33] PolyPt/Ru self-assembles into nanoparticles, which accumulate at tumor sites and are taken up by cisplatin-resistant cancer cells, where it releases cisplatin in the reductive microenvironments. Irradiating PolyPt/Ru with red light generates $^1O_2$ and induces degradation of the Ru(II) moieties, and the release of anticancer Ru(II) complexes. The damage caused by the released Ru(II) complexes and $^1O_2$ are different from those caused by cisplatin, which can eliminate the deactivation pathway via repair.[34] The combination of the released cisplatin and Ru(II) complexes as well as the generated $^1O_2$ has a synergistic effect against cisplatin-resistant tumors. Therefore, PolyPt/Ru can overcome multiple deactivation pathways and reverse cisplatin resistance. Photoactivation of PolyPt/Ru only occurs at the irradiated tumor tissue, which further improves the selectivity of the cancer treatment.

To prepare PolyPt/Ru, we synthesized the Ru(II)-containing monomer $[Ru(biq)_2(PCE)_2](PF_6)_2$ (biq = 2,2'-biquinoline, PCE = propiolic acid 2-[2-[2-(4-cyanophenoxy)ethoxy]ethoxy]ethyl ester) (Figure S1, Supporting Information) and Pt(IV)-containing monomer precursor $[Pt(NH_3)_2Cl_2(AAE)_2](TFA)_2$ (AAE = 3-aminopropionic acid ester, TFA = trifluoroacetic acid) (Figure S2, Supporting Information) via multi-step routes. The monomers and intermediates were fully characterized using nuclear magnetic resonance (NMR) spectroscopy and mass spectrometry (MS) (Figures S4–S15, Supporting Information). Subsequently, the Pt(IV)-containing monomer precursor was deprotonated and polymerized with the Ru(II)-containing monomer via spontaneous amino-yne click polymerization (Figures S3 and S16, Supporting Information). Finally, PolyPt/Ru was synthesized by terminating the polymer with poly(ethylene glycol) methyl ether amine (mPEG5k-NH2) (Figure S3, Supporting Information). NMR spectroscopy and gel permeation chromatography (GPC) demonstrated that PolyPt/Ru was successfully synthesized (Figures S17 and S18, Supporting Information). The molar mass of PolyPt/Ru measured by NMR spectroscopy was 17 kg mol^{-1}, which was comparable to that measured by GPC (18 kg mol^{-1}). The weight fraction of the Pt(IV)/Ru(II) block was ≈42%, indicating that PolyPt/Ru has a high content of anticancer Pt(IV) and Ru(II) moieties.

We prepared the PolyPt/Ru nanoparticles via self-assembly. PolyPt/Ru was dissolved in a THF/DMF mixture. Water was added dropwise to the mixture to trigger the self-assembly. Subsequently, PolyPt/Ru nanoparticles in an aqueous solution were obtained by removing the THF and DMF via dialysis against water. Transmission electron microscopy (TEM) showed that PolyPt/Ru self-assembled into nanoparticles with an average diameter of 90 nm (**Figure 2**a). Dynamic light scattering (DLS) results showed that the PolyPt/Ru nanoparticles had an average hydrodynamic diameter of 111 nm (Figure 2b), which was comparable to the TEM result.

The PolyPt/Ru nanoparticles in aqueous solution were stable for 24 h in the dark (Figure S19, Supporting Information).

The Ru(II) and Pt (IV) moieties in PolyPt/Ru are light- and reduction-responsive, making PolyPt/Ru nanoparticles degradable (Figure 1). We studied the degradation of PolyPt/Ru nanoparticles induced by red light irradiation, GSH treatment, and the combination of red light and GSH treatment using DLS (Figure 2c). The average diameter of the original PolyPt/Ru nanoparticles was 111 nm. After red light irradiation, photoproducts with diameters of 56 and 269 nm appeared. This observation suggested that the PolyPt/Ru nanoparticles degraded into smaller-sized fragments, and some larger-sized hydrophobic aggregates of photoproducts. Similar DLS signals were observed when PolyPt/Ru nanoparticles were treated with GSH. When PolyPt/Ru nanoparticles were treated with a combination of light and GSH, the smaller fragments disappeared, and larger aggregates were formed. TEM observations further confirmed that light or GSH treatments resulted in morphological changes (Figure S20, Supporting Information).

We also performed GPC measurements in a good solvent (DMF), to analyze the degraded products (Figure 2d). The hydrophobic products were easily dissolved in DMF to detect the degraded fragments through GPC. The PolyPt/Ru polymer eluted earlier than the relative degradation products. The delay in the retention time of the products indicated the formation of a series of low-molecular-weight fragments, which confirmed that light and GSH degraded PolyPt/Ru. In addition, UV–vis absorption spectroscopy showed that photosubstitution of the Ru(II) moieties occurred when the PolyPt/Ru nanoparticles were irradiated with red light in the presence or absence of GSH (Figure S21, Supporting Information). Irradiating PolyPt/Ru nanoparticles in the presence of GSH resulted in a faster reaction. This observation indicated that the degradation of Pt(IV) moieties using GSH promoted the photoreactivity of the Ru(II) moieties in the PolyPt/Ru nanoparticles (Figure S22, Supporting Information).

The TEM, DLS, GPC, and UV–vis absorption spectroscopy results demonstrated the qualitative degradation of PolyPt/Ru. PolyPt/Ru degradation is difficult to quantify because the products are complex mixtures. Therefore, $[Ru(biq)_2(PCE)_2](PF_6)_2$ and $[Pt(NH_3)_2Cl_2(AAE)_2](TFA)_2$ were used as model compounds to investigate the reaction mechanism. UV–vis spectroscopy was used to study the photosubstitution of $[Ru(biq)_2(PCE)_2](PF_6)_2$ (Figure 2e). Red light irradiation of $[Ru(biq)_2(PCE)_2](PF_6)_2$ red-shifted the metal-to-ligand charge transfer (MLCT) band from 535 nm (λ_{max} of $[Ru(biq)_2(PCE)_2](PF_6)_2$) to 586 nm ($\lambda_{max}$ of $[Ru(biq)_2(H_2O)_2](PF_6)_2$). The spectral change was achieved within 20 min, suggesting the efficient photosubstitution of $[Ru(biq)_2(PCE)_2](PF_6)_2$. High-performance liquid chromatography (HPLC) was then performed to quantify the photosubstitution of $[Ru(biq)_2(PCE)_2](PF_6)_2$ (Figure 2f). $[Ru(biq)_2(PCE)_2](PF_6)_2$ is represented by the signal peak, 1. After 671 nm light irradiation (125 mW cm^{-2}, 20 min), peak 1 disappeared, and three new peaks, the photoproducts, appeared. Comparing the retention time of the photoproducts with pure PCE ligand confirmed that peak 4 was the PCE. Furthermore, according to the UV–vis absorption spectroscopy detector in the HPLC system, peaks 2 and 3 could be assigned to $[Ru(biq)_2(H_2O)_2](PF_6)_2$ and $[Ru(biq)_2(PCE)(H_2O)](PF_6)_2$, respectively (Figure S23, Supporting Information). The contents of $[Ru(biq)_2(H_2O)_2](PF_6)_2$
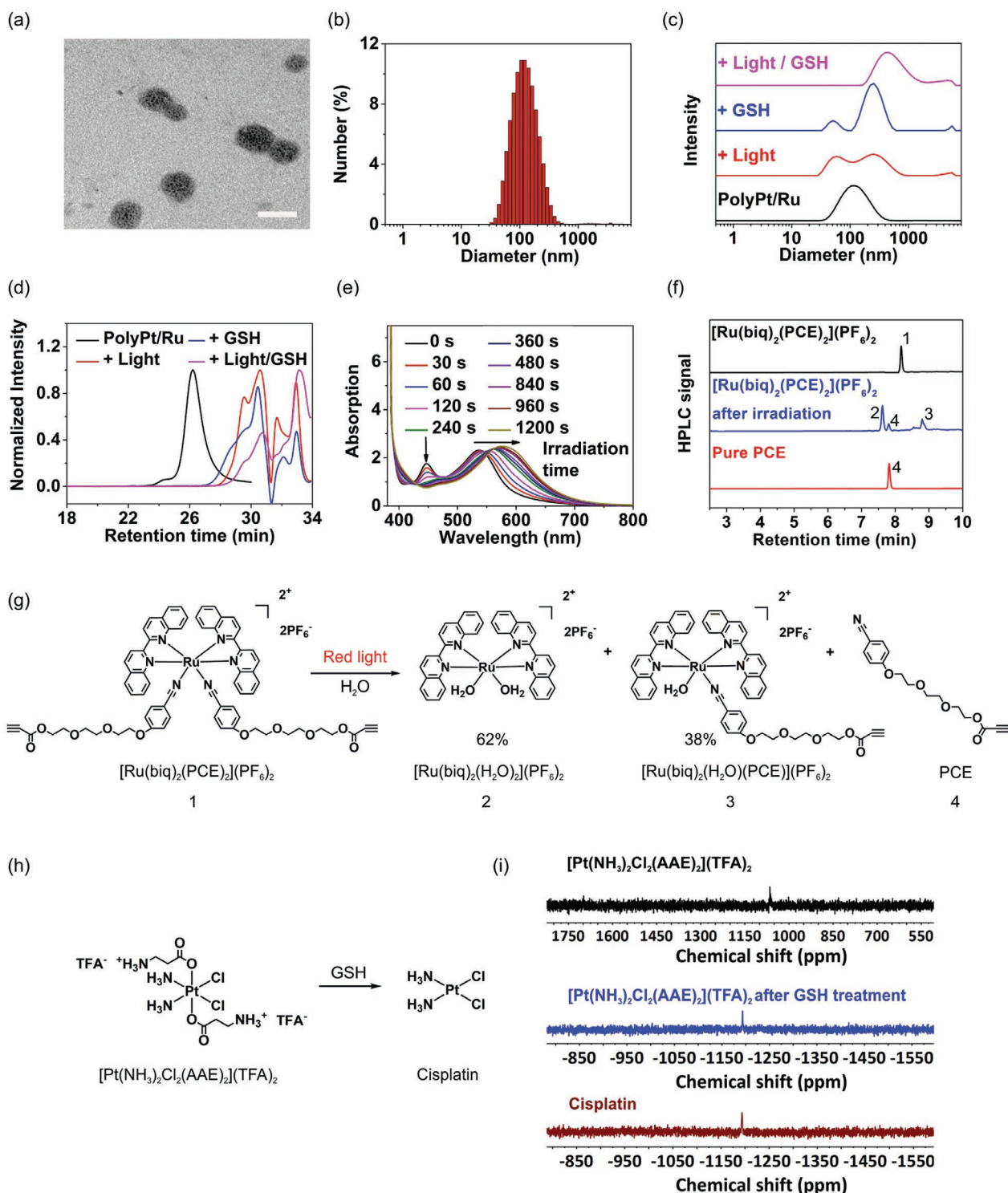
Figure 2. a) A TEM image of PolyPt/Ru nanoparticles. Scale bar: 100 nm. b) The diameter of PolyPt/Ru nanoparticles measured by dynamic light scattering (DLS). c) DLS measurements of PolyPt/Ru nanoparticles. + Light: PolyPt/Ru nanoparticles after light irradiation (671 nm, 125 mW cm^{-2}, 20 min); + GSH (glutathione): PolyPt/Ru nanoparticles after GSH treatment (5.0×10^{-3} M, 4 h); + Light/GSH: PolyPt/Ru nanoparticles after light irradiation (671 nm, 125 mW cm^{-2}, 20 min) with GSH treatment (5.0×10^{-3} M, 4 h). d) GPC traces of PolyPt/Ru. + Light: PolyPt/Ru after light irradiation (671 nm, 125 mW cm^{-2}, 20 min); + GSH: PolyPt/Ru after GSH treatment (5.0×10^{-3} M, 4 h); + Light/GSH: PolyPt/Ru after light irradiation (671 nm, 125 mW cm^{-2}, 20 min) with GSH treatment (5.0×10^{-3} M, 4 h). e) UV–vis absorption spectra of [Ru(biq)$_2$(PCE)$_2$](PF$_6$)$_2$ under light irradiation (671 nm, 125 mW cm^{-2}, 4 h) over time. f) Photosubstitution of [Ru(biq)$_2$(PCE)$_2$](PF$_6$)$_2$ studied by high-performance liquid chromatography (HPLC). [Ru(biq)$_2$(PCE)$_2$](PF$_6$)$_2$ was irradiated using 671 nm light (125 mW cm^{-2}, 20 min). g) Scheme for the photosubstitution of [Ru(biq)$_2$(PCE)$_2$](PF$_6$)$_2$. h) Scheme for the reduction of [Pt(NH$_3$)$_2$Cl$_2$(AAE)$_2$] (TFA)$_2$. i) ^{195}Pt NMR spectra of [Pt(NH$_3$)$_2$Cl$_2$(AAE)$_2$](TFA)$_2$, [Pt(NH$_3$)$_2$Cl$_2$(AAE)$_2$](TFA)$_2$ after GSH treatment (5.0×10^{-3} M, 4 h), and pure cisplatin.

Table 1. Half-maximal inhibitory concentration (IC_{50}) values of cisplatin, $[Pt(NH_3)_2Cl_2(AAE)_2](TFA)_2$ and $[Ru(biq)_2(H_2O)_2](PF_6)_2$ (Figure S24, Supporting Information).

Cell line	Cisplatin	$[Pt(NH_3)_2Cl_2(AAE)_2](TFA)_2$	$[Ru(biq)_2(H_2O)_2](PF_6)_2$		
	IC_{50}[a]	IC_{50}	$IC_{50,dark}$	$IC_{50,light}$	PI[c]
Sensitive A549	16.10 (0.92)[d]	9.38 (0.99)	3.66 (1.02)	2.72 (0.93)	1.34
Sensitive BEL-7404	5.68 (0.86)	4.89 (0.93)	2.97 (0.93)	0.68 (0.19)	4.36
Cisplatin-resistant A549-DDP[b]	100.10 (3.46)	41.80 (0.72)	19.70 (0.94)	5.99 (0.97)	3.28
Cisplatin-resistant 7404-CP20[b]	77.30 (0.96)	35.10 (1.00)	28.70 (1.11)	8.87 (1.09)	3.23

[a]The IC_{50} unit is µg mL^{-1}; [b]Resistance factor (RF) against cisplatin, defined as IC_{50} (resistant cell) against cisplatin/IC_{50} (sensitive cell) against cisplatin. The RF of A549-DDP and 7404-CP20 cells was 6.21 and 13.60, respectively; [c]Phototoxicity index (PI), defined as $IC_{50,dark}/IC_{50,light}$; [d]Standard error of each independent experiment.

and $[Ru(biq)_2(PCE)(H_2O)](PF_6)_2$ were 62% and 38%, which showed that most of the PCE ligands were cleaved from $[Ru(biq)_2(PCE)_2](PF_6)_2$ via red light irradiation (Figure 2g).

The reduction-responsiveness mechanism of $[Pt(NH_3)_2Cl_2(AAE)_2](TFA)_2$ was investigated using ^{195}Pt NMR spectroscopy (Figure 2h,i). The chemical shift of $[Pt(NH_3)_2Cl_2(AAE)_2](TFA)_2$ was located at 1067.1 ppm. The chemical shifts of both cisplatin and the reductive product were located at −1194.7 ppm, suggesting that the reductive product was cisplatin. The ^{195}Pt NMR results showed that $[Pt(NH_3)_2Cl_2(AAE)_2]$ $(TFA)_2$ produced cisplatin via GSH treatment.

Cisplatin released from PolyPt/Ru can inhibit cancer cell growth. The half-maximal inhibitory concentration (IC_{50}) values of cisplatin for the sensitive A549 and BEL-7404 cancer cells were as low as 16.10 and 5.68 µg mL^{-1}, respectively (**Table 1**). These results showed that cisplatin efficiently inhibited the growth of sensitive cancer cells. However, the IC_{50} values of cisplatin for the resistant A549-DDP and 7404-CP20 cancer cells were an order of magnitude higher (Table 1), which indicates that cisplatin is ineffective against resistant cancer cells.

Furthermore, we studied the anticancer performance of $[Pt(NH_3)_2Cl_2(AAE)_2](TFA)_2$, which can produce cisplatin under intracellular reduction environments. The IC_{50} values of $[Pt(NH_3)_2Cl_2(AAE)_2](TFA)_2$ for the sensitive A549 and BEL-7404 cells, and the resistant A549-DDP and 7404-CP20 cells were 41%, 14%, 58%, and 54% lower than those of cisplatin (Table 1), respectively. This indicates that $[Pt(NH_3)_2Cl_2(AAE)_2](TFA)_2$ can inhibit both sensitive and resistant cancer cells more efficiently than cisplatin.

$[Ru(biq)_2(H_2O)_2](PF_6)_2$ released from PolyPt/Ru has anticancer activity against sensitive cancer cells.[35] Its anticancer activity is enhanced via photoirradiation because of $^1O_2$ generation (Figure S25, Supporting Information).[35] Here, we compared its activity against sensitive and resistant cells. In the dark, the IC_{50} values of $[Ru(biq)_2(H_2O)_2](PF_6)_2$ for the sensitive A549 and BEL-7404 cells were 3.66 and 2.97 µg mL^{-1}, respectively (Table 1). Upon red light irradiation, the IC_{50} values of $[Ru(biq)_2(H_2O)_2](PF_6)_2$ for the sensitive cells were as low as 2.72 and 0.68 µg mL^{-1}; the anticancer efficacy of $[Ru(biq)_2(H_2O)_2]$ $(PF_6)_2$ against the sensitive cells was enhanced via photoirradiation because of $^1O_2$ generation. Furthermore, the IC_{50} values of $[Ru(biq)_2(H_2O)_2](PF_6)_2$ for the resistant A549-DDP and 7404-CP20 cells were 19.70 and 28.70 µg mL^{-1} in the dark (Table 1). Upon red light irradiation, the IC_{50} values of $[Ru(biq)_2(H_2O)_2]$ $(PF_6)_2$ for the resistant cells were as low as 5.99 and

8.87 µg mL^{-1}, respectively. The IC_{50} values of $[Ru(biq)_2(H_2O)_2]$ $(PF_6)_2$ for A549-DDP and 7404-CP20 after photoirradiation were 70% and 69% lower than those in the dark, respectively. This demonstrated that $[Ru(biq)_2(H_2O)_2](PF_6)_2$ exhibited enhanced anticancer activity against resistant cancer cells.

The anticancer efficacy of $[Pt(NH_3)_2Cl_2(AAE)_2](TFA)_2$ and $[Ru(biq)_2(H_2O)_2](PF_6)_2$ encouraged us to deliver PolyPt/Ru nanoparticles into cisplatin-resistant cancer cells. We studied the uptake of PolyPt/Ru nanoparticles by cisplatin-resistant cancer cells. Both resistant A549-DDP and 7404-CP20 cells were incubated with PolyPt/Ru nanoparticles for 6 h in the dark. Subsequently, confocal laser scanning microscopy (CLSM) images were taken at 4 and 6 h. The observation of red fluorescence indicated that PolyPt/Ru nanoparticles were efficiently taken up by both resistant cancer cells (**Figure 3**a,b and Figures S27 and S28, Supporting Information). Flow cytometry was used to quantitatively analyze the uptake efficiency of PolyPt/Ru nanoparticles (Figure S26, Supporting Information). After incubation for 6 h, the uptake efficiencies for A549-DDP and 7404-CP20 cells were 76.4% and 54.4%, respectively. These results demonstrated that PolyPt/Ru nanoparticles were efficiently taken up by the cisplatin-resistant cells.

We then investigated the anticancer performance of PolyPt/Ru nanoparticles against cisplatin-resistant cells (Figure 3c,d). In the dark, the cell viabilities decreased as the concentration of the nanoparticles increased. When the equivalent Ru(II) and Pt(IV) concentrations in the nanoparticles were 128 and 40 µg mL^{-1}, the cell viabilities decreased to 31% and 42% for the A549-DDP and 7404-CP20 cells, respectively. We infer that the decrease in cell viability occurred because cisplatin was produced via the reduction of the Pt(IV) moieties in PolyPt/Ru. Moreover, light irradiation further decreased the viability of the cancer cells (Figure 3c,d). The enhanced cytotoxicity was attributed to $^1O_2$ generated and $[Ru(biq)_2(H_2O)_2](PF_6)_2$ released (Figure S28, Supporting Information). The generation of $^1O_2$ in resistant A549-DDP and 7404-CP20 cells was detected using a green fluorescent probe (Figure 3e,f). No green fluorescence was observed in the absence of PolyPt/Ru nanoparticles, the probe, or light irradiation. However, green fluorescence was observed when the cells with PolyPt/Ru nanoparticles and the probe were irradiated with red light. Additionally, the cytotoxicity caused by the release of cisplatin and $[Ru(biq)_2(H_2O)_2](PF_6)_2$, along with the generated $^1O_2$ was notable (Figure S29, Supporting Information). Their synergistic effects reversed cisplatin resistance (Figures S30 and S31, Supporting Information).
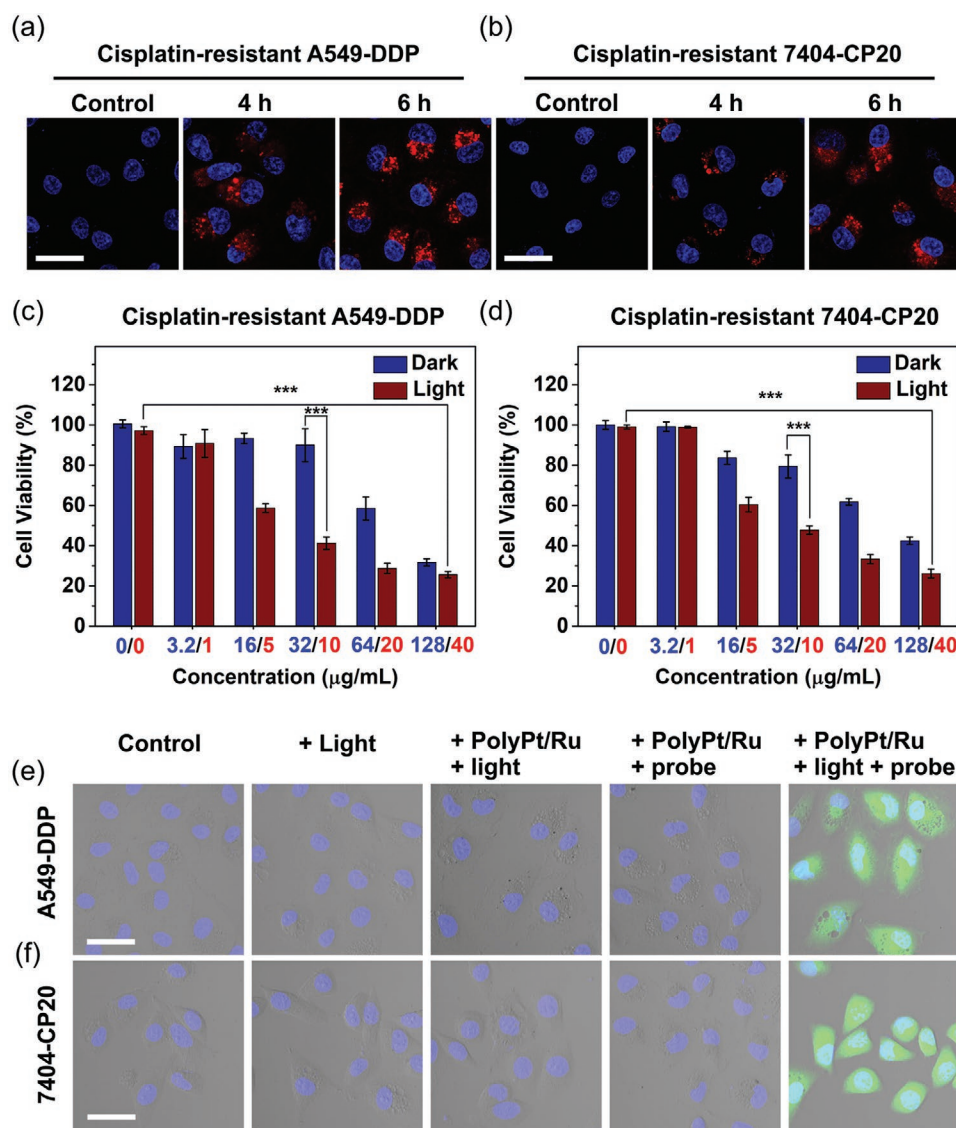
**ADVANCED
SCIENCE NEWS**

www.advancedsciencenews.com

**ADVANCED
MATERIALS**

www.advmat.de

Figure 3. a,b) Confocal laser scanning microscopy (CLSM) images of PolyPt/Ru nanoparticles (red) after incubation with cisplatin-resistant A549-DDP (a) and 7404-CP20 (b) cancer cells for different time periods. Nuclei were stained with Hoechst 33342 (blue). Scale bars: 25 µm. c,d) Viability of cisplatin-resistant A549-DDP (c) and 7404-CP20 (d) cancer cells treated with equivalent Ru(II) and Pt(IV) concentrations in the nanoparticles in the dark and under light irradiation. The equivalent Ru(II) concentration is shown in blue color and the equivalent Pt(IV) concentration is shown in red color. The cells were irradiated with 671 nm red light (125 mW cm^{-2}, 20 min) after incubation with PolyPt/Ru nanoparticles for 6 h. Cell viability was tested after the cells were further incubated in the dark for 24 h. e,f) Generation of intracellular $^1O_2$ in A549-DDP and 7404-CP20 cells as observed by CLSM. The cells were divided into five groups: control group; + light group: cancer cells irradiated with light (671 nm light, 125 mW cm^{-2}, 1 min); +PolyPt/Ru + light group: cancer cells with PolyPt/Ru nanoparticles and light irradiation (671 nm light, 125 mW cm^{-2}, 1 min); +PolyPt/Ru + probe group: cancer cells with PolyPt/Ru nanoparticles and the $^1O_2$ probe; +PolyPt/Ru + light + probe group: cancer cells with PolyPt/Ru nanoparticles, $^1O_2$ probe, and light irradiation (671 nm light, 125 mW cm^{-2}, 1 min). Nuclei were stained with Hoechst 33342 (blue). $^1O_2$ was detected using the indicator DCFH-DA (green). Scale bars: 50 µm.

Encouraged by the anticancer efficacy of PolyPt/Ru nanoparticles in vitro, we studied the anticancer efficacy of PolyPt/Ru nanoparticles in vivo. Hemolysis analysis indicated that PolyPt/Ru nanoparticles have good blood compatibility (Figure S32, Supporting Information). We then investigated the anticancer performance of PolyPt/Ru nanoparticles using a hepatic patient-derived cancer xenograft (PDX) mouse model. PDX models are vastly similar to patient tumors because the tumor tissue is taken from patients and grown in physiologically relevant tumor microenvironments.[36,37] PDX models have been applied in molecular and genetic investigations of drug resistance in previous studies.[38–40]

To study the accumulation of nanoparticles, a PDX-tumor-bearing mouse was intravenously injected with PolyPt/Ru nanoparticles from the tail vein. Fluorescence images of the mouse model (right) and a control mouse (left) were taken over time after injection (**Figure 4**a). No signal and a weak signal were observed at 0 and 4 h in the mouse model, respectively. The fluorescence from PolyPt/Ru nanoparticles at the tumor site reached a maximum at 12 h, which indicated that PolyPt/Ru
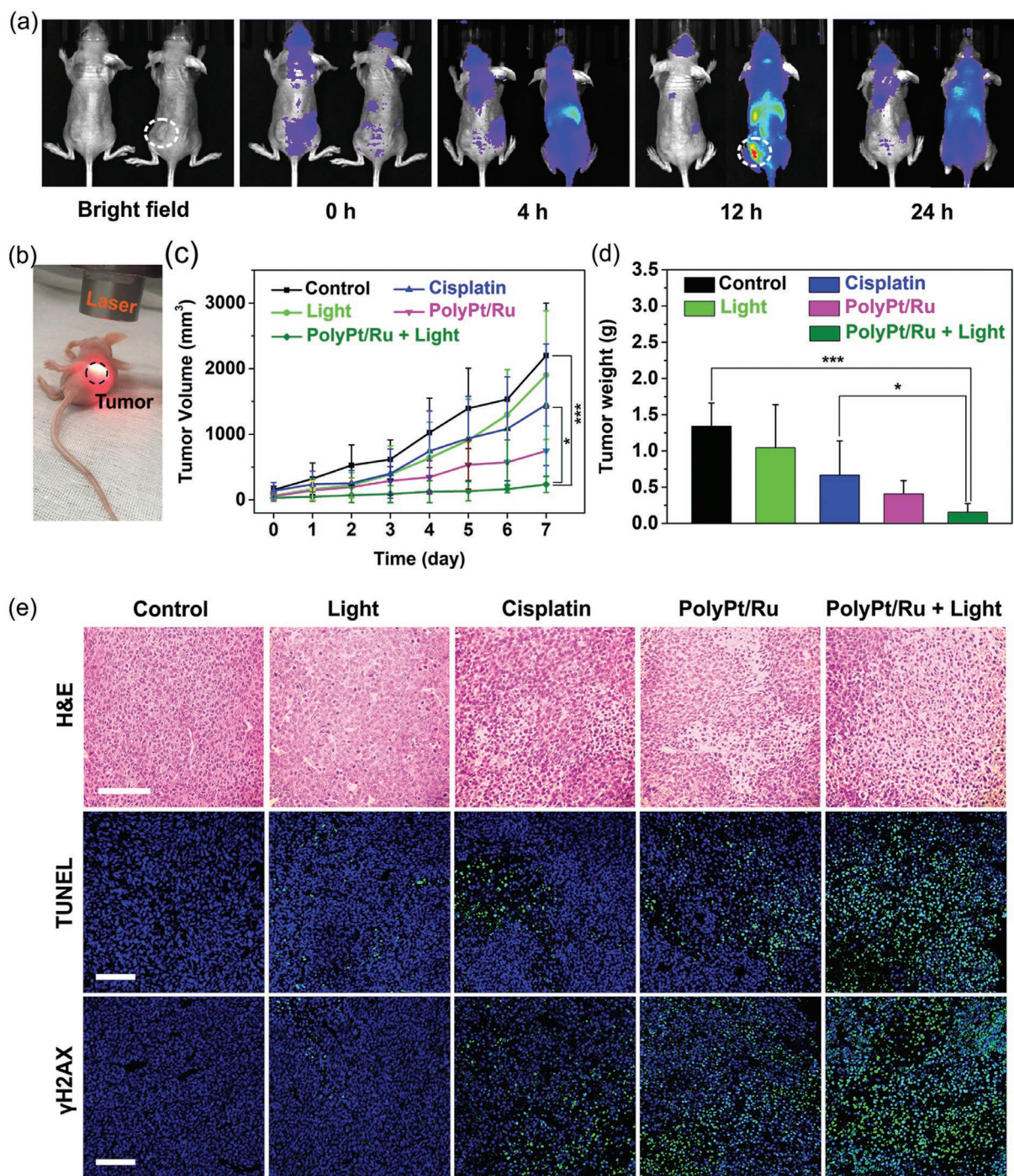
ADVANCED
SCIENCE NEWS
www.advancedsciencenews.com

ADVANCED
MATERIALS
www.advmat.de

Figure 4. a) Fluorescence images of PDX-tumor-bearing mice after intravenous injection of saline (left, control) and PolyPt/Ru nanoparticles (right). Images were taken after injection for 0, 4, 12, and 24 h. The dashed circle indicates the tumor. b) A photograph shows red light irradiation on a mouse model. c) Tumor volumes of PDX-tumor-bearing mice during different treatments. d) Average tumor weights at day 7 after different treatments. e) H&E, TUNEL, and γH2AX staining of tumor sections isolated from the mice on day 7. The damaged DNA strands and γH2AX are labeled by FITC (green). Cell nuclei are stained with DAPI (blue). Scale bars: 100 μm.

nanoparticles efficiently accumulated at the tumor site. The fluorescence intensity at 24 h became weaker, suggesting that the nanoparticles were cleared through metabolism. In contrast, the control mouse injected with saline showed no fluorescence, which proved that the fluorescence was produced by the injected nanoparticles. These experiments demonstrated that PolyPt/Ru nanoparticles accumulate at the tumor site, which we deduced was due to the well-known EPR effect.

Twelve hours after PolyPt/Ru nanoparticles were intravenously injected into the mouse model, the tumor was

irradiated with a 671 nm laser for 20 min (PolyPt/Ru + light group). Four additional experiments were conducted for comparison: 1) PDX-tumor-bearing mice were injected with saline (Control Group); 2) PDX-tumor-bearing mice were irradiated with light (Light Group); 3) PDX-tumor-bearing mice were injected with an equivalent dosage of cisplatin (Cisplatin Group), and 4) PDX-tumor-bearing mice were injected with PolyPt/Ru nanoparticles (PolyPt/Ru Group). We compared the anticancer efficacy by monitoring the tumor volumes of each group over 7 days (Figure 4c). The tumor volume in the control group increased by ≈30 times. The result of the light group was similar to that of the control group, indicating that mild light irradiation does not have an inhibitory effect (Figures S33 and S34, Supporting Information). Cisplatin treatment caused a tumor growth of ≈13 times, since PDX tumors are resistant to cisplatin. For the PolyPt/Ru group, the increase in the tumor volume was smaller (≈8 times) than those in the previous groups. This result indicated that the Pt(IV) moieties in PolyPt/Ru contributed to tumor inhibition. Compared to the four groups mentioned above, tumor growth in the PolyPt/Ru + light group was notably inhibited. This result suggests that the synergistic effects of this treatment improved the anticancer performance.

Subsequently, the mice were euthanized, and the tumors were isolated for analysis (Figure S36, Supporting Information). The average tumor weight in the PolyPt/Ru + light group was much lighter than that in the other four groups (Figure 4d). Immunohistochemical analyses were also performed to illustrate the mechanism of the anticancer activity using PolyPt/Ru nanoparticles (Figure 4e). A hematoxylin and eosin (H&E) staining assay showed large areas of apoptosis and necrosis, which suggested that the PolyPt/Ru + light group treatment exhibited considerable tumor inhibition. Similar results were observed in TUNEL staining images. Furthermore, the γH2AX staining assay provided more insight into the anticancer mechanism since γH2AX is a sensitive marker for DNA damage (Figure S35, Supporting Information). Comparing γH2AX formation at tumor sites, we found that enhanced genomic DNA damage appeared in the PolyPt/Ru + light group. We hypothesized that the released anticancer agents induced DNA damage, which increased genomic instability and apoptosis. Once DNA damage occurs, γH2AX forms clusters near the impaired DNA strands.

We also investigated the systemic toxicity during the treatments by comparing the H&E staining images of the main organs (heart, liver, lung, spleen, and kidney) (Figure S38, Supporting Information). Negligible pathological alteration of the organs was observed, indicating the low systemic toxicity of PolyPt/Ru. The body weights of the mice did not change significantly during the treatments (Figure S39, Supporting Information), which suggests that the treatments had minimal side effects. The combined results demonstrate that the use of PolyPt/Ru can treat PDX tumors with improved efficacy and minimized systemic toxicity.

In conclusion, we synthesized a dual-responsive, bimetallic polymer, PolyPt/Ru, to overcome multiple deactivation pathways for cisplatin. PolyPt/Ru showed excellent performance against cisplatin-resistant tumors due to the design of the polymer structure, and the synergistic effects of the bimetallic moieties. Cisplatin resistance in a PDX model was reversed using PolyPt/Ru. Our study revealed that the design

of multi-metallic polymers with multi-responsiveness is a new strategy to treat drug-resistant cancers. Since many bioactive metal complexes exist, the design principles reported here provide a foundation for the design of multi-metallic polymers for biomedical applications. We anticipate that more multi-metallic polymers with adjustable functions can be developed for personalized nanomedicine and enhanced clinical effectiveness.

The usage of mice, the use of human tissue to establish the PDX model, and all animal procedures were approved by the Animal Care and Use Committee of National Center for Nanoscience and Technology (Approval No. NCNST-PE-AP2019061001).

Supporting Information

Supporting Information is available from the Wiley Online Library or from the author.

Conflict of Interest

The authors declare no conflict of interest.

Keywords

cisplatin, drug resistance, metallodrugs, phototherapy, polymers

[1] T. C. Johnstone, K. Suntharalingam, S. J. Lippard, *Chem. Rev.* **2016**, *116*, 3436.

[2] W. Zhang, J. Shen, H. Su, G. Mu, J.-H. Sun, C.-P. Tan, X.-J. Liang, L.-N. Ji, Z.-W. Mao, *ACS Appl. Mater. Interfaces* **2016**, *8*, 13332.

**ADVANCED
SCIENCE NEWS**

www.advancedsciencenews.com

**ADVANCED
MATERIALS**

www.advmat.de

[3] X.-J. Liang, H. Meng, Y. Wang, H. He, J. Meng, J. Lu, P. C. Wang, Y. Zhao, X. Gao, B. Sun, *Proc. Natl. Acad. Sci. USA* **2010**, *107*, 7449.

[4] M. D. Hall, M. Okabe, D.-W. Shen, X.-J. Liang, M. M. Gottesman, *Annu. Rev. Pharmacol. Toxicol.* **2008**, *48*, 495.

[5] G. Ferraro, L. Massai, L. Messori, A. Merlino, *Chem. Commun.* **2015**, *51*, 9436.

[6] S. Li, C. Li, S. Jin, J. Liu, X. Xue, A. S. Eltahan, J. Sun, J. Tan, J. Dong, X.-J. Liang, *Biomaterials* **2017**, *144*, 119.

[7] Y. Min, C. Q. Mao, S. Chen, G. Ma, J. Wang, Y. Liu, *Angew. Chem., Int. Ed.* **2012**, *124*, 6846.

[8] J. Hu, J. D. Lieb, A. Sancar, S. Adar, *Proc. Natl. Acad. Sci. USA* **2016**, *113*, 11507.

[9] Z. Wang, Z. Xu, G. Zhu, *Angew. Chem., Int. Ed.* **2016**, *55*, 15564.

[10] W. H. Ang, I. Khalaila, C. S. Allardyce, L. Juillerat-Jeanneret, P. J. Dyson, *J. Am. Chem. Soc.* **2005**, *127*, 1382.

[11] X. Ling, X. Chen, I. A. Riddell, W. Tao, J. Wang, G. Hollett, S. J. Lippard, O. C. Farokhzad, J. Shi, J. Wu, *Nano Lett.* **2018**, *18*, 4618.

[12] M. Stilgenbauer, A. M. Jayawardhana, P. Datta, Z. Yue, M. Gray, F. Nielsen, D. J. Bowers, H. Xiao, Y.-R. Zheng, *Chem. Commun.* **2019**, *55*, 6106.

[13] Y. H. Kim, S. W. Shin, B. S. Kim, J. H. Kim, J. G. Kim, Y. J. Mok, C. S. Kim, H. S. Rhyu, J. H. Hyun, J. S. Kim, *Cancer* **1999**, *85*, 295.

[14] J. Karges, T. Yempala, M. Tharaud, D. Gibson, G. Gasser, *Angew. Chem., Int. Ed.* **2020**, *59*, 7069.

[15] M. Michalak, M. S. Lach, M. Antoszczak, A. Huczyński, W. M. Suchorska, *Molecules* **2020**, *25*, 537.

[16] Y. Zheng, D. Y. Zhang, H. Zhang, J. J. Cao, C. P. Tan, L. N. Ji, Z. W. Mao, *Chem. - Eur. J.* **2018**, *24*, 18971.

[17] R. K. Pathak, S. Dhar, *J. Am. Chem. Soc.* **2015**, *137*, 8324.

[18] Z.-T. Cao, Z.-Y. Chen, C.-Y. Sun, H.-J. Li, H.-X. Wang, Q.-Q. Cheng, Z.-Q. Zuo, J.-L. Wang, Y.-Z. Liu, Y.-C. Wang, *Biomaterials* **2016**, *94*, 9.

[19] R. Xing, Q. Zou, C. Yuan, L. Zhao, R. Chang, X. Yan, *Adv. Mater.* **2019**, *31*, 1900822.

[20] J. Li, D. Cui, Y. Jiang, J. Huang, P. Cheng, K. Pu, *Adv. Mater.* **2019**, *31*, 1905091.

[21] M. Abbas, Q. Zou, S. Li, X. Yan, *Adv. Mater.* **2017**, *29*, 1605021.

[22] X. Xu, P. E. Saw, W. Tao, Y. Li, X. Ji, S. Bhasin, Y. Liu, D. Ayyash, J. Rasmussen, M. Huo, *Adv. Mater.* **2017**, *29*, 1700141.

[23] L. Zeng, P. Gupta, Y. Chen, E. Wang, L. Ji, H. Chao, Z.-S. Chen, *Chem. Soc. Rev.* **2017**, *46*, 5771.

[24] C. Mari, V. Pierroz, S. Ferrari, G. Gasser, *Chem. Sci.* **2015**, *6*, 2660.

[25] L. N. Lameijer, T. G. Brevé, V. H. van Rixel, S. H. Askes, M. Siegler, S. Bonnet, *Chem. - Eur. J.* **2018**, *24*, 2709.

[26] W. Sun, R. Thiramanas, L. D. Slep, X. Zeng, V. Mailänder, S. Wu, *Chem. - Eur. J.* **2017**, *23*, 10832.

[27] G. Carrone, L. Zayat, L. D. Slep, R. Etchenique, *Phys. Chem. Chem. Phys.* **2017**, *19*, 2140.

[28] L. Zayat, C. Calero, P. Alborés, L. Baraldo, R. Etchenique, *J. Am. Chem. Soc.* **2003**, *125*, 882.

[29] L. N. Lameijer, D. Ernst, S. L. Hopkins, M. S. Meijer, S. H. Askes, S. E. Le Dévédec, S. Bonnet, *Angew. Chem., Int. Ed.* **2017**, *129*, 11707.

[30] M. H. Al-Afyouni, T. N. Rohrabaugh, K. F. Al-Afyouni, C. Turro, *Chem. Sci.* **2018**, *9*, 6711.

[31] P. del Pino, F. Yang, B. Pelaz, Q. Zhang, K. Kantner, R. Hartmann, N. Martinez de Baroja, M. Gallego, M. Möller, B. B. Manshian, *Angew. Chem., Int. Ed.* **2016**, *128*, 5573.

[32] A. Salvati, A. S. Pitek, M. P. Monopoli, K. Prapainop, F. B. Bombelli, D. R. Hristov, P. M. Kelly, C. Åberg, E. Mahon, K. A. Dawson, *Nat. Nanotechnol.* **2013**, *8*, 137.

[33] J. Chen, J. Ding, Y. Wang, J. Cheng, S. Ji, X. Zhuang, X. Chen, *Adv. Mater.* **2017**, *29*, 1701170.

[34] B. S. Howerton, D. K. Heidary, E. C. Glazer, *J. Am. Chem. Soc.* **2012**, *134*, 8324.

[35] W. Sun, S. Li, B. Häupler, J. Liu, S. Jin, W. Steffen, U. S. Schubert, H. J. Butt, X. J. Liang, S. Wu, *Adv. Mater.* **2017**, *29*, 1603702.

[36] Y. Cong, H. Xiao, H. Xiong, Z. Wang, J. Ding, C. Li, X. Chen, X. J. Liang, D. Zhou, Y. Huang, *Adv. Mater.* **2018**, *30*, 1706220.

[37] L. Rao, G. T. Yu, Q. F. Meng, L. L. Bu, R. Tian, L. S. Lin, H. Deng, W. Yang, M. Zan, J. Ding, *Adv. Funct. Mater.* **2019**, *29*, 1905671.

[38] K.-T. Kim, H. W. Lee, H.-O. Lee, S. C. Kim, Y. J. Seo, W. Chung, H. H. Eum, D.-H. Nam, J. Kim, K. M. Joo, *Genome Biol.* **2015**, *16*, 127.

[39] C. A. Stewart, C. M. Gay, Y. Xi, S. Sivajothi, V. Sivakamasundari, J. Fujimoto, M. Bolisetty, P. M. Hartsfield, V. Balasubramaniyan, M. D. Chalishazar, *Nat. Cancer* **2020**, *1*, 423.

[40] O. Poirion, X. Zhu, T. Ching, L. X. Garmire, *Nat. Commun.* **2018**, *9*, 4892.

2004766 (9 of 9)